Environmental Research 159 (2017) 466–473

Contents lists available at ScienceDirect

Environmental Research

journal homepage: www.elsevier.com/locate/envres

Long-term atmospheric visibility trends in megacities of China, India and the United States

Yue Hu[a], Ling Yao[b], Zhen Cheng[c], Yungang Wang[d,*]

[a] College of Environment and Civil Engineering, Chengdu University of Technology, Chengdu 610059, China
[b] Institute of Geographic Sciences and Natural Resources Research, Chinese Academy of Sciences, Beijing 100101, China
[c] School of Environmental Science and Engineering, Shanghai Jiao Tong University, Shanghai 200240, China
[d] GAGO Inc., 1601 McCarthy Blvd., Milpitas, CA 95035, USA

A R T I C L E I N F O

Keywords:
Atmospheric visibility
Air quality
Aerosol optical depth
Air pollution
Public health

A B S T R A C T

Millions of premature deaths worldwide every year mostly in China and India are contributed by the poor air quality. The atmospheric visibility is a proven indicator of the ambient air quality. In this study, nine megacities were selected, including Beijing, Shanghai and Guangzhou from China, Chicago, Los Angeles (LA) and New York City (NYC) from the United States, and Mumbai, Chennai and Jaipur from India. The data of visibility, aerosol optical depth (AOD), and meteorological factors from 1973 to 2015 were collected. The temporal variations of annual and monthly percentages of bad days (visibility < 5 km) and good days (visibility > 15 km) were evaluated. Visibility of Chicago, LA and NYC gradually improved during the past 43 years and has reached a very good level (good day percentages: 75–88%; bad day percentages: 0 – 4%). Conversely, visibility in Mumbai, Chennai and Jaipur continued deteriorating and suffered an extremely poor visibility situation in recent years (good day percentages: 0; bad day percentages: 6–100%). Likewise, visibility in Beijing, Shanghai and Guangzhou has experienced the worsening period during the industrial development from 1970s and turned better after the 1990s. A strong seasonal pattern of bad day percentages of each year were observed in most cities, especially in the winter, which is caused by the fossil fuel combustion for heating, relatively high relative humidity, and other unfavorable meteorological conditions. The low visibility events occurred more frequently in days with low wind speeds and specific wind directions, further explaining the seasonal patterns of visibility. With population growth from the period of 2000–2010 to the period of 2011–2015, AOD and bad day percentages both increased in Mumbai, Chennai, Jaipur and Beijing while others were relatively stable. This study demonstrated that the macro-control of pollution emissions could effectively reduce air deterioration. The relationships among visibility variation, meteorological, pollutant and population factors provide valuable scientific support for public health researches, air quality managements (monitoring and forecasting), and clean energy initiatives.

1. Introduction

The atmospheric visibility is defined as the maximum horizontal distance, at which the threshold of a target object can be recognized against the background by human eyes (Deng et al., 2012; Horvath, 1981). High visibility (> 100 km) can be observed in unpolluted circumstances with clear weather while low visibility would be often attributed to heavy air pollution and bad meteorological conditions (Deng et al., 2012; Zhao et al., 2011). The visibility could decrease due to the scattering and absorption of visible light by particles and gases in the atmosphere (Watson and Chow, 2006; Hyslop, 2009), and the patterns of air pollution are exactly massive emissions of particle and gas pollutants into the air. Furthermore, it is known that the emission of particulate pollutants can cause visibility impairment, which makes the visibility an important proxy for the particulate matter pollution (Clancy et al., 2002; Kim et al., 2006). Although visibility can be impacted by specific meteorological phenomena such as high wind speeds, rainfall and fog events, the long-term influence of meteorological conditions is relatively stable (Zhao et al., 2011). Therefore, the long-term trend of visibility can indicate the variation of air pollution status (Chen and Xie, 2013; Fu et al., 2014).

Due to rapid industrial developments and economic growth, human beings have paid great environmental costs for serious air pollution issues, which could heavily damage public health (Zhang et al., 2010).

* Corresponding author.
E-mail address: carl@gagogroup.com (Y. Wang).

http://dx.doi.org/10.1016/j.envres.2017.08.018
Received 30 March 2017; Received in revised form 7 August 2017; Accepted 9 August 2017
0013-9351/

The United States, China and India are three of the most populated countries in the world with vast territories. They all have been experiencing significant industrial developing processes. In the past decades, because of the industrial revolution and significant environmental improvement, atmospheric visibility of the U.S. cites decreased before 1970s and then increased, which has the most serious sulfur and organics pollution in the mid-eastern and western urban regions (Davis, 1991; Malm, 1992; Malm and Molenar, 1984; Malm et al., 1994; Schichtel et al., 2001). As a result of population and economic explosions in Indian cities, the associated air pollution cause significant declines of visibility over a hundred years (Dani et al., 2012; De et al., 2005; Jaswal et al., 2013; Tiwari et al., 2011). In the most populated areas of China such as the North China Plain and the Pearl River Delta, evident visibility falling on account of air pollution attracted a large number of researchers investigating the visibility trends and relationships with meteorological factors and other pollutants (Deng et al., 2012, 2008; Fu et al., 2014; Gao et al., 2011; Zhang et al., 2010; Zhao et al., 2011). Hence, the understanding of the mechanism of visibility variations plays a key role in air pollution emergency response and regional air quality management.

In this study, three megacities from the three countries including China, the U.S. and India were chosen. These nine cities are Beijing, Shanghai, Guangzhou, New York City (NYC), Chicago, Los Angeles (LA), Mumbai, Chennai and Jaipur (Fig. 1). These cities are the most economically developed, populated and represent different geographic and meteorological conditions of each country. From 1973 to 2015, the annual visibility variations were investigated. Relationships between visibility and meteorological factors (relative humidity, wind speed and wind direction), social economic parameters and the aerosol optical depth (AOD) were discussed. Studying the long-term trends of visibility in populated cities with the consideration of impacts of human activities is valuable for smart urban planning.

2. Data and methodology

Beijing, Shanghai, Guangzhou, Chicago, NYC, LA, Mumbai, Chennai and Jaipur were chosen as the representative cities from China, the U.S. and India, respectively (Fig. 1), which were selected from ten most populated cities of each country. With complete time series of datasets from 1973 to 2015, the top three populated cites were determined. Visibility and other meteorological parameters including the wind speed, wind direction, air temperature and dew-point temperature of these nine cities with at least 3 h intervals from 1973 to 2015 were collected from the National Climate Data Center (NCDC) (Data source: http://www1.ncdc.noaa.gov/pub/data/noaa/). The units of visibility datasets are miles, which was converted into kilometers. Although the NCDC is highly authoritative that provides global weather and climate data, there are non-negligible uncertainties of original datasets caused by various factors such as the conversion of observation methods. Hence a series of processes were performed to obtain data, which could accurately reflect relationships between visibility and air pollution.

To minimize the influences caused by meteorological factors, low visibility observations due to specific weather conditions such as mist, precipitation and fog were removed, which generally have high relative humidity (RH) and could not represent status of air pollution (Che et al., 2007; Chen and Xie, 2013). With RH changing, the diameter and refractive index will change because hydrophilic aerosols absorb water vapor. It is defined as the aerosol hygroscopicity, which reflected as the variation of visibility in the horizontal direction (Liu et al., 2012; Tang, 1996). Therefore, visibility data with RH < 90% in the range from 9:00 a.m. to 6:00 p.m. (local time) were chosen for screening, cleaning and further long-term trend analysis (Section 3.1). RH was calculated through the equation (Linsley et al., 1988):

$$RH = 100 \times \left(\frac{112 - 0.1T + T_d}{112 + 0.9T}\right)^8$$

where T (°C) represents the air temperature and T_d represents (°C) the dew point temperature. In addition, the SYNOP (Surface Synoptic Observations) and METAR (Meteorological Terminal Air Report) standards of visibility observation were mixed together in original datasets. METAR data are encoded by automated airport weather stations and SYNOP data are encoded by both manned and automated weather stations. These two types of records have different observation standards, that the upper limit of METAR is 10 miles while observations of SYNOP could reach 30 miles or higher (many observations with values of 100 miles were recorded) (Li et al., 2016). Moreover, the time resolution of SYNOP is 3 h and METAR is 1 h or half an hour. To compensate the influences caused by METAR records, only monitoring

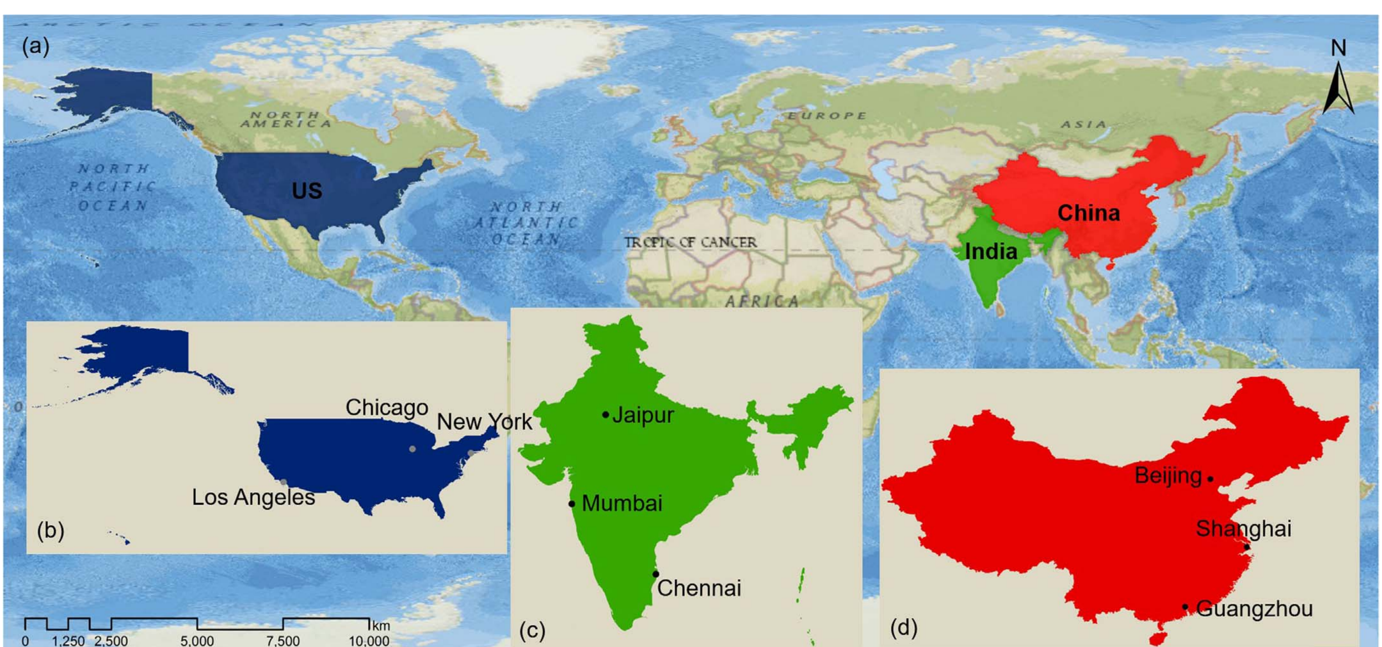

Fig. 1. **(a)** Locations of China, the United States and India on the world map; **(b)** Locations of Chicago, Los Angeles and New York City in the US; **(c)** Locations of Mumbai, Chennai and Jaipur in India; **(d)** Locations of Beijing, Shanghai and Guangzhou in China.

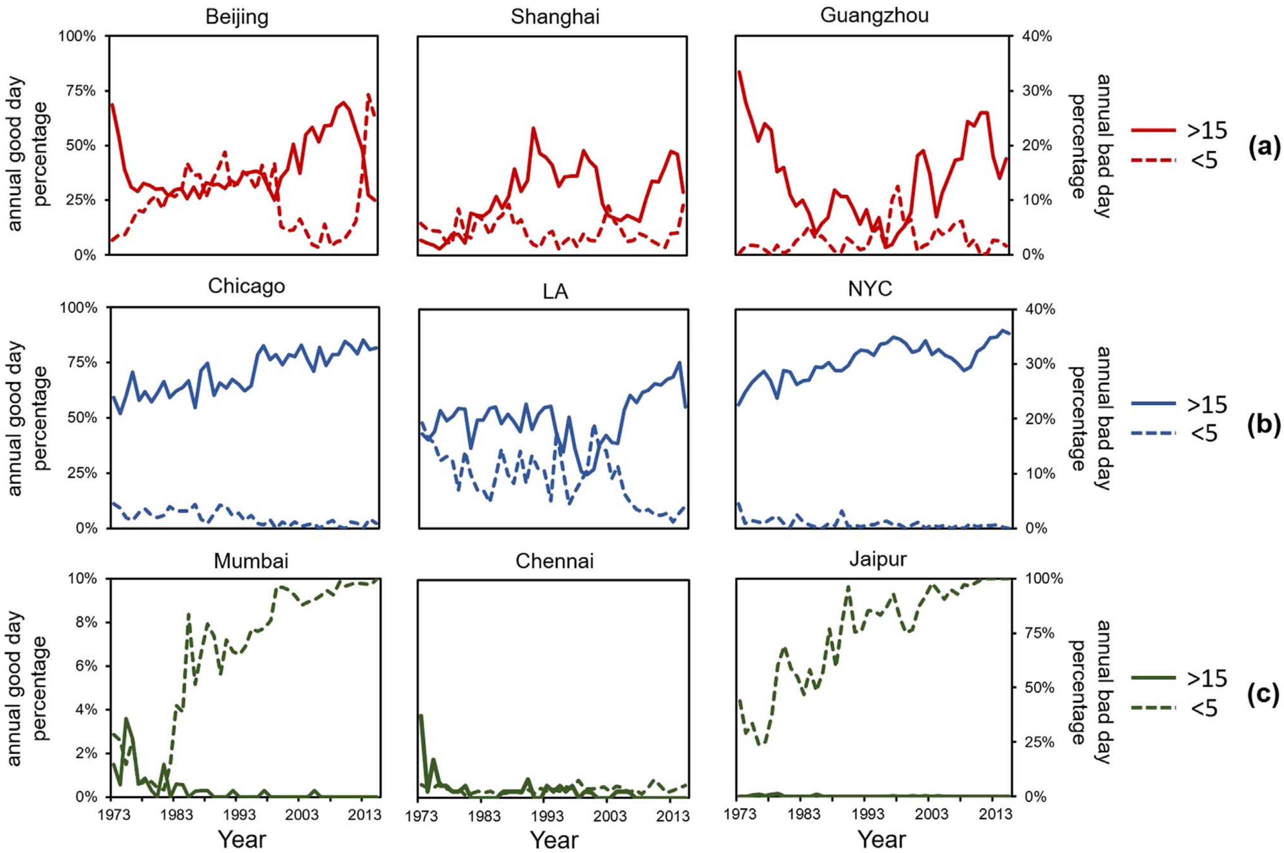

Fig. 2. Long-term variations of the annual good (visibility > 15 km) and bad (visibility < 5 km) day percentages of based on visibility of nine populated cities in **(a)** China, **(b)** U.S. and **(c)** India. Solid lines represent the good day percentage while dashed lines represent the bad day percentage.

stations at airports and data at integral points with 3 h intervals from 9:00 a.m. to 6:00 p.m. were selected (see supplementary information Table 1 for station lists of each city), during which time the possibility of fog and mist are relatively lower in the whole day. Calculating daily average values then obtaining the annual medians of visibility was the widely accepted method for the long-term visibility trend analysis (Gao et al., 2011; Lee, 1988). However, METAR observations almost occupied the whole period after late 1990s of American cities, and maintained good air quality for most of the time (with 10 miles records), leading to a sharp decrease of annual median visibility (see supplementary information Fig. S1 for example). Thus, we decide to use percentages of good days (daily mean visibility > 15 km) and bad days (daily mean visibility < 5 km) of each year for each city instead, to demonstrate the long-term trends of visibility, which could more accurately indicate the long-term variation of air pollution (Chen and Xie, 2013; Gomez and Smith, 1987). Furthermore, the bad visibility frequency was calculated directly based on the data points, instead of daily mean values of visibility. These two results were used in the following analysis interpreting relationships between visibility and other variables.

The aerosol optical depth (AOD) of major cities all over the world from 2000 to 2015 was derived from the MODIS products MOD04 and MYD04, carried on satellites Terra and Auqa. The resolution of our AOD data (sub-satellite point) were 3 km × 3 km. Original datasets were extracted from corresponding pixels of MOD04 and MYD04, calculating mean values of pixel values after removing filling values, which were recorded when no data was observed. Then the mean values were used as the daily average AOD. If no available observation was found during an entire day, null values were used for the daily average AOD values. Likewise, correlations between AOD and visibility were performed using nonparametric Kendall rank correlation test, because visibility data were not normal distributed. The significant level, α, was set at 0.05. The correlation coefficient τ and P values were presented. To explore relationships between urbanization and air pollution, population data of each city at each year were collected. The population data of cities in U.S. and China were both downloaded from the national bureau of statistics (http://www.stats.gov.cn/). And Indian population data were collected from this website: http://www.indiaonlinepages.com/population/index.html.

3. Results and discussion

3.1. Long-term visibility trend

The long-term trends of annual percentages of good and bad visibility days demonstrated different characteristics among cities and countries (Fig. 2), which indicated different government attitudes towards the air quality. In Fig. 2, it is easy to sort these three countries according to their situations of visibility: U.S. cities > Chines cities > Indian cities. Cities of each country have demonstrated different patterns of long-term visibility variation. Indian cities have experienced much more low visibility conditions in the past 43 years compared to the U.S. and China.

In China, Beijing had apparent higher percentages of bad days (1.4–29.3%) compared to Shanghai (1.2–9.3%) and Guangzhou (0 – 12.6%) (Fig. 2a). Between 1973 and late 1990s, the good and bad day percentages of Beijing decreased then increased, respectively. It indicates the continuously heavy air pollution caused by industrial emissions found in previous studies (Fu et al., 2014; Zhao et al., 2011). From 1998–2008, the visibility substantially improved partially due to the "Blue Sky Project" for hosting the 2008 Beijing Olympic Games. During this project, the daily average PM_{10} Air Quality Index (AQI) was reduced from 81 to 44 (Zhang et al., 2010) through limiting emissions from coal and biomass combustion in the surrounding areas of Beijing,

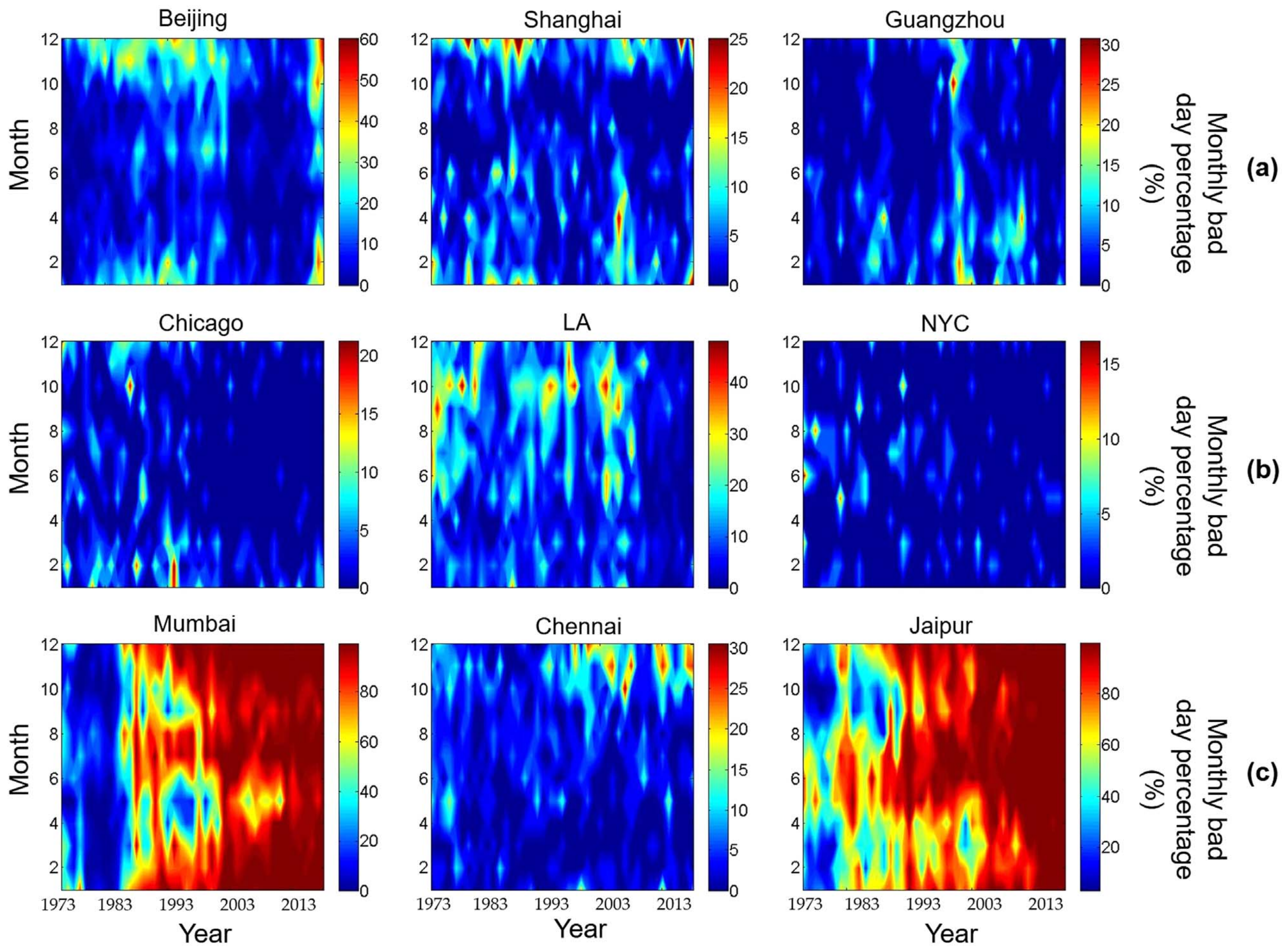

Fig. 3. The monthly distribution of the bad day percentage from 1973 to 2015 at cities of **(a)** China, **(b)** U.S. and **(c)** India. The color represents fractional distribution of bad day percentages of each month. (For interpretation of the references to color in this figure legend, the reader is referred to the web version of this article.).

which were reported the two largest contributing factors of low visibility (Chang et al., 2009; Zhao et al., 2011). However, after 2008, with private cars booming and the deregulation of air pollution emissions, visibility sharply deteriorated (the bad day percentage increased from 1.7% to 29.3%), causing the public alarm and making headlines of many international medias (Fig. 2a). For Shanghai, the bad day percentages fluctuated and reached peaks at 1987 (9.3%), 2003 (9.0%) and 2015 (9.2%) then stayed at a relatively low level for the rest of the time. However, the good day percentages declined from 58.1% to 15.8% during 1991–2008, which could be explained by the air pollution emissions associated with the rapid economic growth and industrial development (Chang et al., 2009; Gao et al., 2011). The bad day percentages of Guangzhou increased from 1973 (0.3%) to 1998 (12.6%) then declined to 2015 (1.6%), while the good day percentage declined sharply from 1973 (83.6%) to late 1990s (3.5%) then increased to 2010s (65.0%). It coincided with the increasing industrial emissions caused by the Open Policy and the Economic Reform in 1978 and the environmental protection policy aiming at controlling acid rains since 1998 (Chang et al., 2009).

Comparing to the three cities in China, the trends of good and bad day percentages of the other six cities showed fewer fluctuations. The visibility of Chicago, LA and NYC starts improving since 1970s, with good day percentages obviously increasing and bad day percentages declining (Fig. 2b), which reflected the effect of government environmental protection measures such as Clean Air Act in the 1960s, 1970s, and 1990s (Belden, 2001; Chestnut and Dennis, 1997). By comparison, it was evident that the air pollution abatement of LA did not work as well as Chicago and NYC. As one of the most air polluted cities, LA was suffering fine particulate matter (PM) and ozone pollutions, with frequent sunny days and low precipitation accelerating ozone formation, as well as secondary PM (Baldassare et al., 2011). In 2005, a grant program entitled “Diesel Emissions Reduction Act (DERA)” was authorized to improve the air quality by retrofitting diesel engines (Congress, 2005). DERA had conspicuous effect in LA (with bad day percentages dropping from 19% to 3% and good day percentages increasing from 24% to 76%) after it was implemented (Fig. 2b). The visibility improvement (good day percentages exceeded 75% in recent years) of Chicago and NYC also benefited from curtailing air pollution by the U.S. government.

In India, the visibility in Mumbai, Chennai and Jaipur reflected bad air quality condition caused by diversified pollutant sources, which were dominated by coal and biomass combustion in Jaipur (Dani et al., 2012; Jaswal et al., 2013) and mainly identified as vehicle emission, industries, fuel combustion, and construction pollutions in Mumbai and Chennai (Guttikunda et al., 2014; Kumar et al., 2001; Patankar and Trivedi, 2011). Good day percentages of all three Indian cities maintained less than 5% during most of the time and bad day percentages of Mumbai and Jaipur both even reached as high as 100% after 2010 (Fig. 2c). The bad day percentage trends of Mumbai and Jaipur were similar, which constantly increased from 1970s to 2010s, indicating continued emissions of pollutants and the invalid environmental policy in these years. However, the bad day percentage of Chennai kept below 10% and the good day percentage was below 1% after 1975, respectively, suggesting long periods of “general bad visibility” and the different visibility levels between Chennai and other two Indian cities.

Fig. 3 depicts the temporal distribution of the monthly bad day

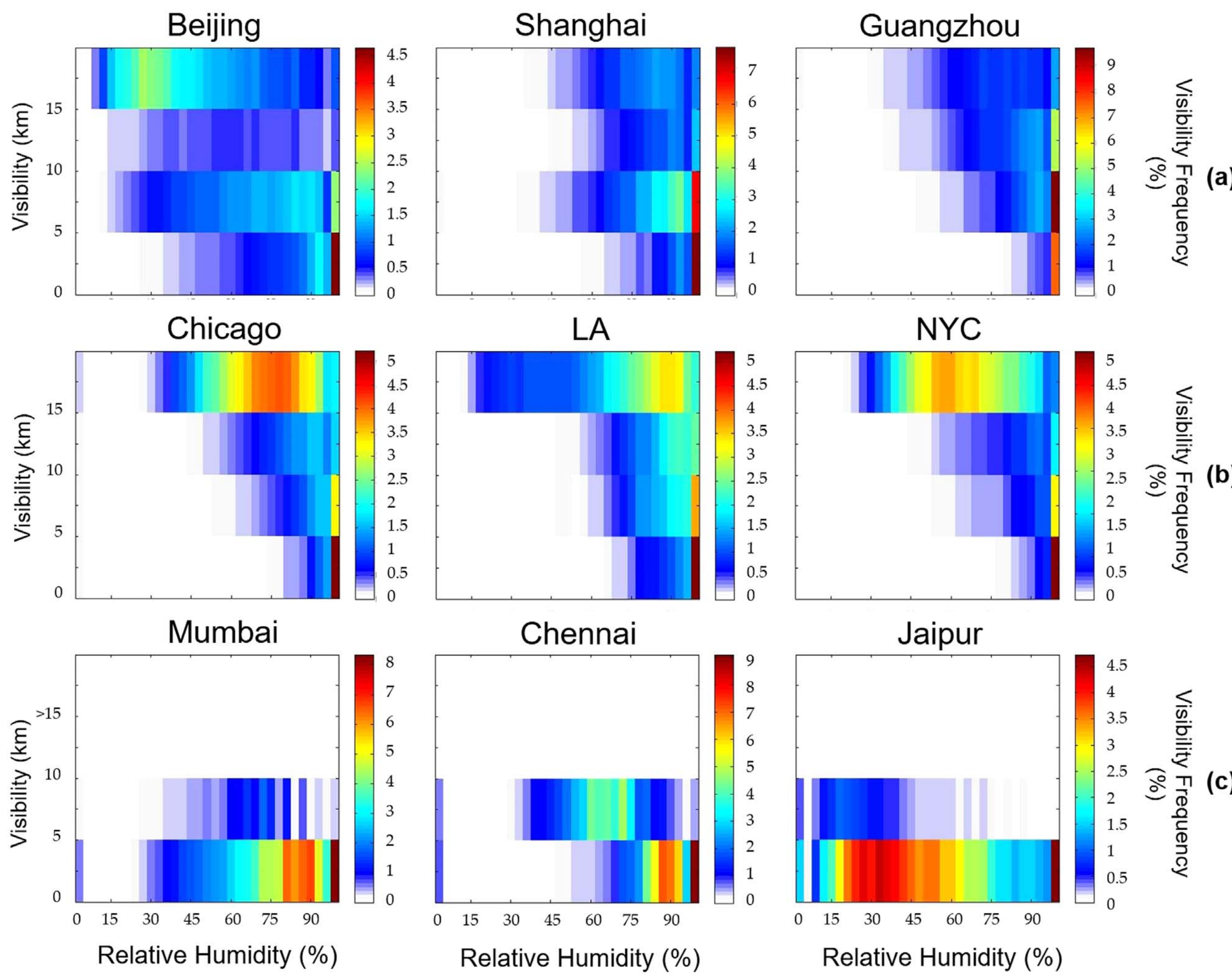

Fig. 4. Occurrence frequency of hourly bad visibility in regard to RH in cities of **(a)** China, **(b)** U.S. and **(c)** India from 1973 to 2015. The visibility was classified into four levels: 0–5 km, 5–10 km, 10–15 km, > 15 km. The RH was divided into 33 categories. The color of each grid represents the occurrence frequency of hourly bad visibility at specific visibility level and RH category. The right bottom corners of each subfigure indicate low visibility in weather conditions like rain and fog, which generally bring about RH > 100%. (For interpretation of the references to color in this figure legend, the reader is referred to the web version of this article.).

percentages of each city. In Chinese cities, Beijing had relatively higher bad day percentages in winter (Dec-Jan) and summer (Jun-Jul) indicating the coal-combustion residential heating in the winter and the aerosol scattering efficiency and the secondary sulfate in the summer, where the aerosol scattering efficiency was accelerated by high ambient RH in summer (Chang et al., 2009; Fu et al., 2014; Zhao et al., 2011). The high bad day percentage values of Shanghai and Guangzhou both occurred in the winter (Dec-Feb) and spring (Apr-Jun). The low temperature in the winter could weaken the air circulation. RH during the pre-monsoon season (spring) is relatively high and the wind direction around both Shanghai and Guangzhou are mostly northwest, where the air pollutants derived from populated inland areas (Gao et al., 2011; Lin et al., 2014; Shi et al., 2014; Wang et al., 2011). The monthly bad day percentage of Chicago and NYC remained low values and did not exhibit any obvious seasonal trend (Fig. 3b). The bad day percentages of LA had higher values in autumn (Sep-Nov), which was primarily due to the high RH and enhanced air pollutants emissions from sources at the western upwind direction during this time (Hildemann et al., 1994). Analogously, all Indian cities showed peaked values in the winter (Oct-Jan), in the consequence of biomass combustion in Jaipur and domestic fuel combustion for heating in Mumbai and Chennai (Guttikunda et al., 2014; Kumar et al., 2001; Patankar and Trivedi, 2011). Likewise, high bad day percentages of Mumbai and Jaipur in the monsoon season (Jun-Aug) might be also influenced by the higher aerosol scattering efficiency based on higher ambient RH compared to other seasons.

3.2. Relationships between visibility and meteorological factors

The relationships of occurrence frequency of hourly bad visibility versus RH and wind direction can further explain the long-term and monthly distributions of bad visibility in each city. Fig. 4 exhibits the occurrence frequency of hourly visibility in relative to RH. The highest occurrence frequency for all nine cities all appear at the lower right corners (with RH > 90%) of each subfigure, indicating the presence of specific weather conditions (e.g. fog and rain). The colors of strips at each visibility classification were good indicators of various visibility conditions. Beijing, Chicago, LA and NYC had highlight strips (yellow-red colors) at high visibility level (> 15 km), reflecting relatively better visibility conditions than others in the past 43 years. Mumbai, Chennai and Jaipur include no data at good visibility levels (> 15 km) and have yellow-red colors in low visibility strips (0–5 km) (Fig. 4c). Focusing on bad visibility strips (visibility < 5 km), hot spots mainly appeared in high RH regions, which were observed in cities of Beijing, Shanghai, Guangzhou, LA, Mumbai and Chennai. It is consistent with the finding of high bad day percentages of these cities in wet seasons (summer in Beijing, Shanghai, Mumbai and Jaipur, and autumn in LA) (Cheung et al., 2011).

Furthermore, the wind rose plots reveal relationships of bad

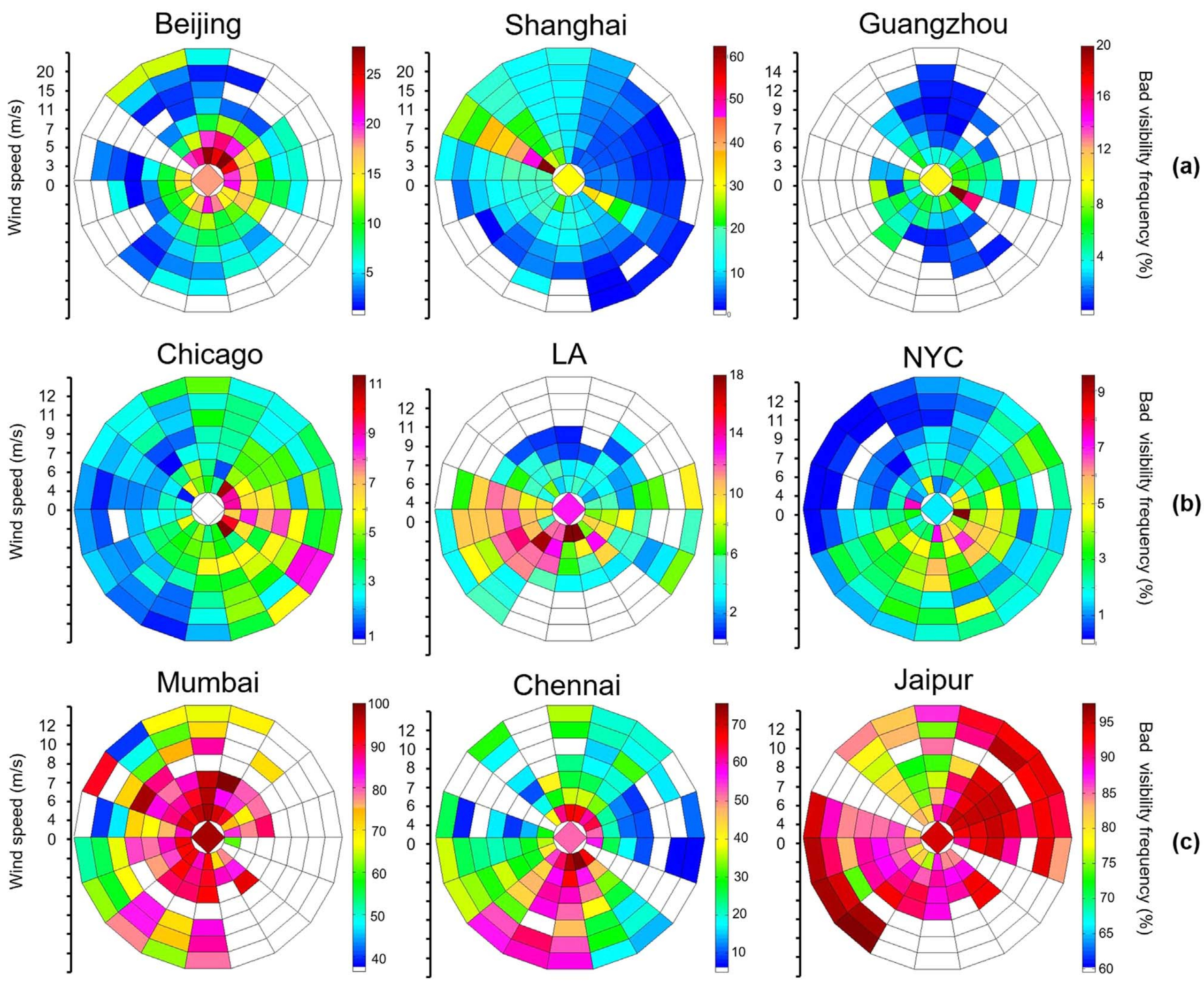

Fig. 5. The bad visibility frequency in relative to wind speed and wind direction in cities of **(a)** China, **(b)** the U.S. and **(c)** India. The radius of each subplot represents the wind speed while the angle of each grid represents the wind direction. The color of each grid represents the bad visibility frequency. (For interpretation of the references to color in this figure legend, the reader is referred to the web version of this article.).

visibility frequency with wind speed and wind direction (Fig. 5). The bad visibility frequency concentrates in low wind speeds in cities including Beijing and Guangzhou suggesting that local emissions were the main contributors. It is in line with the explanation above that severe convective condition under high wind speeds is beneficial for air pollutants dispersion (Chen and Xie, 2013; Zhang et al., 2010). On the other side, bad visibility frequencies also condense in specific wind direction ranges, which is evident in cities of Beijing, Shanghai, Guangzhou, Chicago, LA, Chennai and Jaipur. Because large seasonal variation of wind direction was observed in most selected cities, wind rose plots further elucidates local air pollutants emission sources and the monthly change of bad day percentage. For instance, LA sits in a large basin with the Pacific Ocean to the West, and it is under the typical etesian climate with western winds scraping in the autumn. Therefore, the air pollutants emitted from the large industrial park located to the west were transported to LA (Hildemann et al., 1994). It is confirmed by the fact that LA had high bad day percentage values during September to November (Fig. 2b).

3.3. Relationship between visibility and AOD

Relationships between annual AOD and bad day percentage between 2000 and 2015 are shown in Fig. 6. The variation of AOD can effectively reflect air pollution levels to some extent (Wang et al., 2011; Zhang, 2010). Positive correlations in LA ($\tau = 0.64$, $P < 0.001$), Mumbai ($\tau = 0.62$, $P < 0.001$) and Jaipur ($\tau = 0.70$, $P < 0.001$) were discovered, which were coincident with the fact that air pollution was the key factor of visibility degradation in these cities (Hildemann et al., 1994; Venkataraman et al., 2002). Other cities did not demonstrate significant correlations between annual AOD and bad day percentage, mainly due to the non-neglected disturbance caused by meteorological factors, which were most likely supposed to be the RH (Wu et al., 2012) (see Supplementary information Fig. S2).

Fig. 7 presents the comparison of average bad visibility frequencies between 2000–2010 and 2010–2015, considering both AOD and population in these cities. At first glance, bubbles in the figure were clearly divided into three groups by country. The population boom and deterioration of AOD and visibility were observed in cities of developing countries. On the other side, relatively better status of U.S. cities was kept well. Specifically, Jaipur, Mumbai and Chennai had the highest bad visibility frequency values while Shanghai had the highest AOD values. Shanghai is one of the representative areas with high AOD values caused by massive air pollution emissions and unfavorable meteorological conditions (Huang et al., 2012). However, the slightly decreased average bad visibility frequency values in Shanghai after 2010 (from 14.4% to 10.4%) were also observed. After 2000, population booms in Jaipur and Chennai were obvious, along with bad visibility frequencies and AOD increasing. Likewise, both Mumbai and

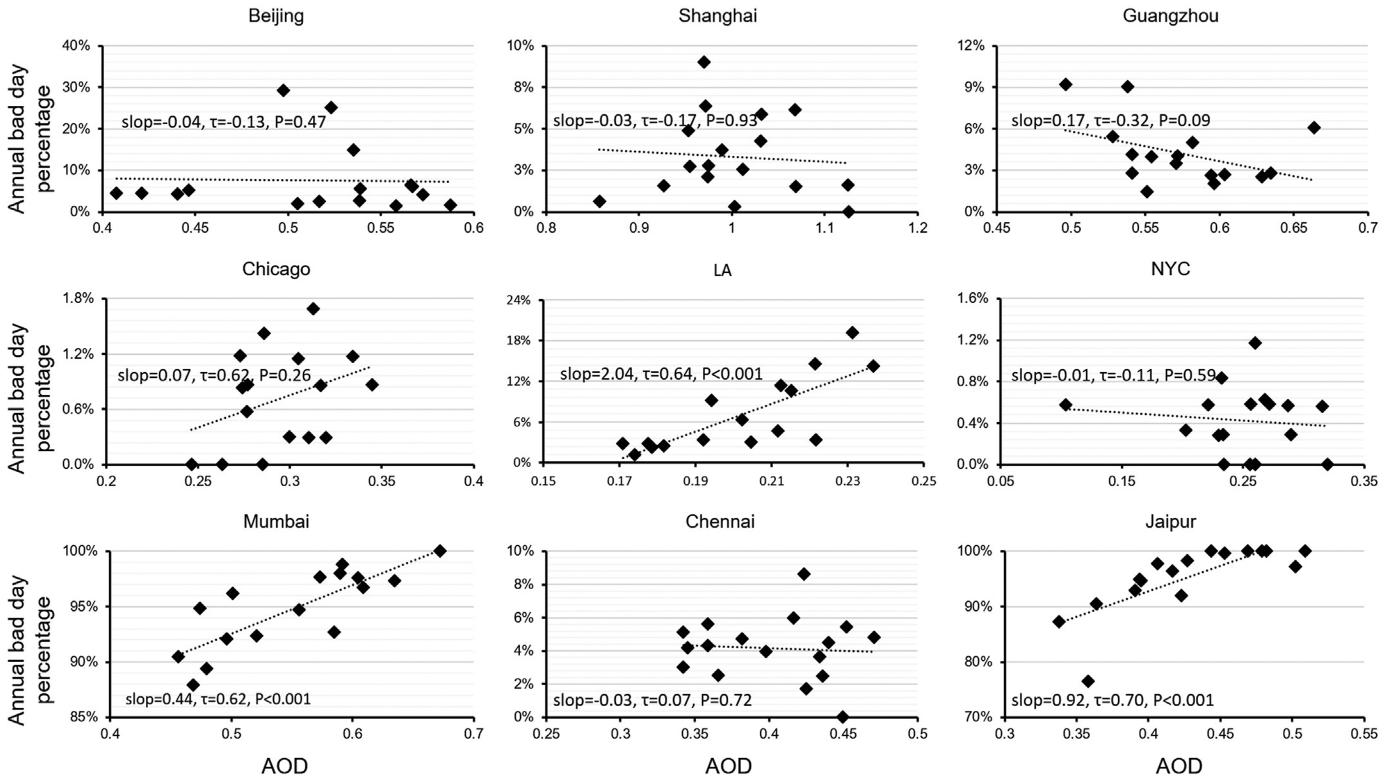

Fig. 6. Correlations between the annual bad day percentage and AOD in cities from 2000 to 2015.

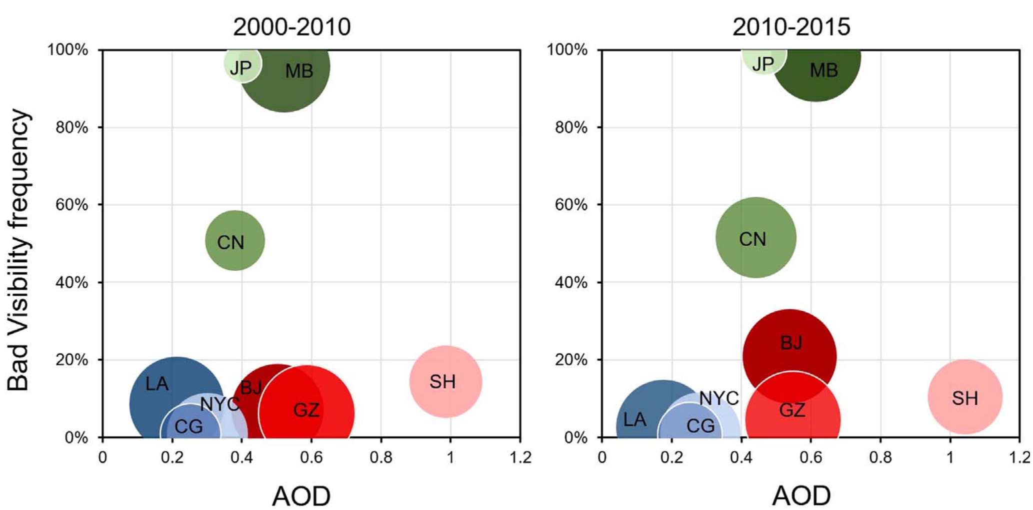

Fig. 7. Comparisons of the bad visibility frequencies in terms of AOD and population in Beijing (BJ), Shanghai (SH), Guangzhou (GZ), Chicago (CG), LA, NYC, Mumbai (MB), Chennai (CN) and Jaipur (JP) between **(a)** 2000 – 2010 and **(b)** 2010 – 2015. The x and y axis represent AOD and bad visibility frequencies, respectively. The size of bubbles represents the population of each city.

Beijing display increased AOD values and bad visibility frequencies, although populations remain stable. U.S. cities show relatively stable status in terms of population, visibility and AOD except for a noticeable visibility improvement for LA. To some extent, it indicated that substantial industrial development, fast-growing number of private vehicles, and significant population growth in recent two decades of these two developing countries have paid the price of great air pollution, contributing to the increase of bad visibility frequencies and AOD, Taking into account of the seriousness of the air pollution, how to develop economy at a lower environmental cost is very severe for India and China.

4. Conclusion

During the past four decades, the long-term trend of atmospheric visibility of selected megacities clearly depicted impacts of air pollutants emissions and various pollution control strategies. Chicago, NYC and LA have successfully gone through the stage of rapid economic development with the cost of environmental deterioration and return good air quality condition again. After the industrial development in the 1970s, visibility in Chinese megacities rapidly decreased and improved with implementing air quality protection policies since late 1990s, reflecting that China is taking the old road of the treatment after pollution. However, one of the main sources of air pollution in Mumbai, Chennai and Jaipur is coal and biomass combustion, which is difficult to control in the current development of India. In addition, the increasing population these years in these cities further enhanced the air pollutant emission intensity from this source. Hence, the air quality of these three cities was all getting degraded and did not exhibit any sign of improvement, which requires economic developments and enough policy makers' attention. The temporal variations of the annual bad visibility day percentages of Chicago, LA and NYC indicate that the reduction of air pollutants emissions could effectively impair the hostile air quality. The control of coal and biomass combustion, vehicle exhaust, and industrial emissions could lead to significant improvement in atmospheric visibility in selected cities.

Acknowledgements

We thank Professor Jing Li at Peking University for the help with data analysis.

Appendix A. Supporting information

Supplementary data associated with this article can be found in the online version at http://dx.doi.org/10.1016/j.envres.2017.08.018.

References

Baldassare, M., Bonner, D., Petek, S., Shrestha, J., 2011. PPIC statewide survey: Californians and the environment. Public Policy of California, San Francisco.
Belden, R.S., 2001. Clean Air Act. Section of Environment, Energy & Resources. American Bar Association, Chicago.
Chang, D., Song, Y., Liu, B., 2009. Visibility trends in six megacities in China 1973–2007. Atmos. Res. 94, 161–167.
Che, H., Zhang, X., Li, Y., Zhou, Z., Qu, J.J., 2007. Horizontal visibility trends in China 1981–2005. Geophys. Res. Lett. 34, L24706.
Chen, Y., Xie, S. d., 2013. Long-term trends and characteristics of visibility in two megacities in southwest China: Chengdu and Chongqing. J. AirWaste Manag. 63, 1058–1069.
Chestnut, L.G., Dennis, R.L., 1997. Economic benefits of improvements in visibility: acid rain provisions of the 1990 Clean Air Act Amendments. J. Air Waste Manag. 47, 395–402.
Cheung, K., Daher, N., Kam, W., Shafer, M., Ning, Z., Schauer, J., Sioutas, C., 2011. Spatial and temporal variation of chemical composition and mass closure of ambient coarse particulate matter (PM 10–2.5) in the Los Angeles area. Atmos. Environ. 45, 2651–2662.
Clancy, L., Goodman, P., Sinclair, H., Dockery, D.W., 2002. Effect of air-pollution control on death rates in Dublin, Ireland: an intervention study. Lancet 360, 1210–1214.
U.S. Congress, 2005. Energy Policy Act of 2005. Public Law, pp. 109–158.
Dani, K., Raj, P., Devara, P., Pandithurai, G., Sonbawne, S., Maheskumar, R., Saha, S., Rao, Y., 2012. Long-term trends and variability in measured multi-spectral aerosol optical depth over a tropical urban station in India. Int. J. Climatol. 32, 153–160.
Davis, R.E., 1991. A synoptic climatological analysis of winter visibility trends in the mideastern United States. Atmos. Environ. B-Urb. 25, 165–175.
De, U., Dube, R., Rao, G., 2005. Extreme weather events over India in the last 100 years. J. Ind. Geophys. Union. 9, 173–187.
Deng, J., Du, K., Wang, K., Yuan, C., Zhao, J., 2012. Long-term atmospheric visibility trend in Southeast China, 1973–2010. Atmos. Environ. 59, 11–21.
Deng, X., Tie, X., Wu, D., Zhou, X., Bi, X., Tan, H., Li, F., Jiang, C., 2008. Long-term trend of visibility and its characterizations in the Pearl River Delta (PRD) region, China. Atmos. Environ. 42, 1424–1435.
Fu, G., Xu, W., Yang, R., Li, J., Zhao, C., 2014. The distribution and trends of fog and haze in the North China Plain over the past 30 years. Atmos. Chem. Phys. 14, 11949–11958.
Gao, L., Jia, G., Zhang, R., Che, H., Fu, C., Wang, T., Zhang, M., Jiang, H., Yan, Peng, 2011. Visual range trends in the Yangtze River Delta region of China, 1981–2005. J. AirWaste Manag. 61, 843–849.
Gomez, B., Smith, C., 1987. Visibility at Oxford, 1926–1985. Weather 42, 98–106.
Guttikunda, S., Rahul, G., Pallavi, P., 2014. Nature of air pollution, emission sources, and management in the Indian cities. Atmos. Environ. 95, 501–510.
Hildemann, L.M., Mazurek, M., Cass, G., Simoneit, B., 1994. Seasonal trends in Los Angeles ambient organic aerosol observed by high-resolution gas chromatography. Aerosol Sci. Technol. 20, 303–317.
Horvath, H., 1981. Atmospheric visibility. Atmos. Environ. 15, 1785–1796 (1967).
Huang, W., Tan, J., Kan, H., Zhao, N., Song, W., Song, G., Chen, G., Jiang, L., Jiang, C., Chen, R., Chen, B., 2012. Visibility, air quality and daily mortality in Shanghai, China. Sci. Total Environ. 407, 3295–3300.
Hyslop, N.P., 2009. Impaired visibility: the air pollution people see. Atmos. Environ. 43, 182–195.
Jaswal, A.K., Kumar, N., Prasad, A.K., Kafatos, M., 2013. Decline in horizontal surface visibility over India (1961–2008) and its association with meteorological variables. Nat. Hazards 68, 929–954.
Kim, Y.J., Kim, K.W., Kim, S.D., Lee, B.K., Han, J.S., 2006. Fine particulate matter characteristics and its impact on visibility impairment at two urban sites in Korea: Seoul and Incheon. Atmos. Environ. 40, 593–605.
Kumar, A., Patil, R., Nambi, K., 2001. Source apportionment of suspended particulate matter at two traffic junctions in Mumbai, India. Atmos. Environ. 35, 4245–4251.
Lee, D., 1988. The choice of visibility statistics in the analysis of long term visibility trends in southern England. Weather 43, 332–338.
Li, J., Li, C., Zhao, C., Su, T., 2016. Changes in surface aerosol extinction trends over China during 1980–2013 inferred from quality-controlled visibility data. Geophys. Res. Lett. 43, 8713–8719.
Lin, Y., Huang, K., Zhuang, G., Fu, J., Wang, Q., Liu, T., Deng, C., Fu, Q., 2014. A multi-year evolution of aerosol chemistry impacting visibility and haze formation over an Eastern Asia megacity, Shanghai. Atmos. Environ. 92, 76–86.
Linsley, R.K., Kohler, M., Paulhus, J., 1988. Hydrology for Engineers. McGraw-Hill, New York, pp. 340.
Liu, X., Zhang, Y., Cheng, Y., Hu, M., Han, T., 2012. Aerosol hygroscopicity and its impact on atmospheric visibility and radiative forcing in Guangzhou during the 2006 PRIDE-PRD campaign. Atmos. Environ. 60, 59–67.
Malm, W.C., 1992. Characteristics and origins of haze in the continental United States. Earth-Sci. Rev. 33, 1–36.
Malm, W.C., Molenar, J.V., 1984. Visibility measurements lo National Parks In the Western United States. Japca J. Air Waste Ma. 34, 899–904.
Malm, W.C., Sisler, J., Huffman, D., Eldred, R., Cahill, T., 1994. Spatial and seasonal trends in particle concentration and optical extinction in the United States. J. Geophys. Res-Atmos. 99, 1347–1370.
Patankar, A., Trivedi, P., 2011. Monetary burden of health impacts of air pollution in Mumbai, India: implications for public health policy. Public Health 125, 157–164.
Schichtel, B.A., Husar, R., Falke, S., Wilson, W., 2001. Haze trends over the United States, 1980–1995. Atmos. Environ. 35, 5205–5210.
Shi, Y., Chen, J., Hu, D., Wang, L., Yang, X., Wang, X., 2014. Airborne submicron particulate (PM_1) pollution in Shanghai, China: chemical variability, formation/dissociation of associated semi-volatile components and the impacts on visibility. Sci. Total Environ. 473, 199–206.
Tang, I.N., 1996. Chemical and size effects of hygroscopic aerosols on light scattering coefficients. J. Geophys. Res. 101, 19245–19250.
Tiwari, S., et al., 2011. Visibility degradation during foggy period due to anthropogenic urban aerosol at Delhi, India. Atmos. Pollut. Res. 2, 116–120.
Venkataraman, C., Reddy, C., Josson, S., Reddy, M., 2002. Aerosol size and chemical characteristics at Mumbai, India, during the INDOEX-IFP (1999). Atmos. Environ. 36, 1979–1991.
Wang, Y., Wan, Q., Meng, W., Liao, F., Tan, H., Zhang, R., 2011. Long-term impacts of aerosols on precipitation and lightning over the Pearl River Delta megacity area in China. Atmos. Chem. Phys. 11, 12421–12436.
Watson, J.G., Chow, J.C., 2006. Visibility and air pollution. WIT Trans. Ecol. Environ. 99, 645–649.
Wu, J., Fu, C., Zhang, L., Tang, J., 2012. Trends of visibility on sunny days in China in the recent 50 years. Atmos. Environ. 55, 339–346.
Zhang, Q., Zhang, J., Xue, H., 2010. The challenge of improving visibility in Beijing. Atmos. Chem. Phys. 10, 7821–7827.
Zhang, R., 2010. Getting to the critical nucleus of aerosol formation. Science 328, 1366–1367.
Zhao, P., Zhang, X., Xu, X., Zhao, X., 2011. Long-term visibility trends and characteristics in the region of Beijing, Tianjin, and Hebei, China. Atmos. Res. 101, 711–718.